The 2009 IEEE/RSJ International Conference on
Intelligent Robots and Systems
October 11-15, 2009 St. Louis, USA

Enhanced Manipulator's Safety with Artificial Pneumatic Muscle

Tae-Yong Choi, Byoung-Suk Choi, Masanori Sugisaka and Ju-Jang Lee, *Fellow*, IEEE

Abstract— **The safety of humans working with robots is an important issue. Many studies have addressed related methods, but fundamental limits to meet required safety have been met owing to the absence of compliance in the robot actuators. Pneumatic muscle is considered to be a basic actuator and offers the advantage of intrinsic elasticity to achieve the joint compliance. Here, the joint compliance actuated by pneumatic muscle is actively utilized to enhance human safety during collisions. To this end, the authors present a novel approach to control compliance and position independently without affecting on the each other's performance using pneumatic muscles. The presented method is verified by experiments using a physical robot.**

I. Introduction

Many robots have been developed to help human beings such as the service robot and industrial robots. As such, close interaction with humans is required. As a result, the requirement of safety as well as traditional metrics of performance must be considered. Accordingly, much research related to safe robots has been reported. In order to avoid collision with obstacles, Graham et al. [1] and Karlsson et al. [2] used a sensor fusion method to detect high-risk obstacles in working space. Ohashi et al. [3] used the humanoid's arms to avoid collisions in a manner similar to human motion. However, the most serious injury or hazard results from the collisions when the collision avoidance methods fail.

Improvements to reduce injury in collisions can be realized with mechanical design. This paper also address the method to reduce injury in collisions. About this problem, Zinn et al. [4] proposed a new actuation mechanism, in which the actuator is divided into low and high frequency terms to reduce the stiffness of the manipulator effectively. Hirzinger et al. [5] developed the light-weight manipulator to decrease inertia. However, the attempts listed above inevitably employed such complex mechanisms and controllers with various sensors due to the absence of a compliance property in actuators. This is related to the use of motors as basic actuators. There is limit to achieve joint compliance when using motors, which have to use gears due to weak torque [6].

To overcome the drawbacks of conventional approaches, Pneumatic Muscle(PM) has been investigated, as it is considered an attractive actuator in terms of providing a safety characteristic. PM offers a high ratio of torque with respect to weight and size, making it possible to actuate machines without resorting to gears. Among various aspects, PM's intrinsic elasticity is its most attractive property with respect to achieving compliance in various applications. In the case of walking robots, PM's elasticity is made use of to allow natural walking [7]–[9]. In the case of an exoskeleton type wearer, PM is used for the shoulder blades in the humanoid [10]. PM's compliance property is utilized for an exoskeleton type wearer for a proposed therapy machine [11]. However, there has been relatively little work involving the use of PM to address safety issues.

The novel joint compliance adjusting method using PMs to increase safety is proposed here by adding a independent joint compliance controller(IJCC) to the position controller to control manipulator's position and compliance simultaneously. The added IJCC provide enhanced safety in collisions through on-line control of the joint compliance. The total controller was composed of the IJCC and the position controller. Compliance from the IJCC has no direct effect on the manipulator's position, but vibration caused by joint compliance results in position errors. Suppressing vibration at PM actuation is almost impossible in practical terms owing to the numerous unpredictable perturbations of position control such as PM model parameter's variation and errors. In particular, PM characteristics are affected by temperature, humidity, and operational stress. In conventional researches related to PM, a sliding mode controller(SMC) has been considered to be the most suitable position controller with respect to minimizing the effort for complex error dynamics [12]–[14]. In particular, Van Damme et al. [13] used Kikuuwe et al. [18]'s Proxy-Based SMC(PBSMC) to increase safety of their manipulator actuated by pleated pneumatic artificial muscle(PPAM). However, it has big disadvantage of low tracking performance because of its delayed positioning.

In the present works, boundary layer augmented SMC (BASMC) is used for position control with mitigated chattering, while securing reasonable positioning performance even with large joint compliance from IJCC. Finally, the safety of both human and robot in the case of collisions is advanced by increased joint compliance with small positioning errors.

This paper is arranged as follows. Section II derives the dynamics of a 2-link manipulator based on a numerical PM model. In addition, the joint compliance characteristic is studied. Section III describes the control method for a robot actuated by PMs. BASMC is used for positioning with IJCC. Section IV gives experimental results for user safety during collision. Section V concludes this work.

T.-Y. Choi, B.-S. Choi and J.-J. Lee are with the Division of Electrical Engineering, School of Electrical Engineering and Computer Science, KAIST, 373-1, Guseong-dong, Yuseong-gu, Daejeon, Korea
taeyongchoi@kaist.ac.kr, bschoi@kaist.ac.kr and jjlee@ee.kaist.ac.kr

M. Sugisake is with the Department of Mechanical and Electrical Engineering, Nippon Bunri University, 1727 Oaza Itiki, Oita, Japan
ms@alife-robotics.co.jp

II. System Modeling

A. Numerical modeling of PM

A PM's mathematical model is necessary to adapt it to use in a robot manipulator. The PM's nonlinearity has been a challenging problem and some advanced models such as [15]–[17] have been suggested. Among them, [16] proposed an easy model to apply to robots with PMs. The dynamic behavior of a PM hanging vertically and actuating a mass has been modeled as a combination of nonlinear friction, a nonlinear spring and a nonlinear contraction, as in (1).

$$M\ddot{x} + B(P)\dot{x} + K(P)\cdot x = F(P) - Mg. \tag{1}$$

$$\begin{aligned} K(P) &= K_0 + K_1 P \ (N/m) \\ B(P) &= \begin{cases} B_{0i} + B_{1i}P \ (N/m/s) \ (inflation) \\ B_{0d} + B_{1d}P \ (N/m/s) \ (deflation) \end{cases} \\ F(P) &= F_0 + F_1 P \ (N). \end{aligned} \tag{2}$$

where $x(t)$ means the amount of PM contraction, with $x = 0$ corresponding to the fully deflated or relaxed PM. P mean pressure. M is a hanging mass. $K(P)$, $B(P)$, $F(P)$ are spring constant, damping constant and elemental contraction force by PM without spring and damping characteristic, and modeled as (2). The coefficient of friction B depends on whether the PM is being inflated or deflated. By rearranging (1), a equation of motion for a mass M is given like (3).

$$F_M = M\cdot a = F(P) - B(P)\dot{x} - K(P)\cdot x \tag{3}$$

where F_M is a given force to a mass M. a or $\ddot{x} + g$ is the acceleration term of the mass M.

Here, the form of (3) is used as the base model. Most researchers agree on PM's fundamental elements, such as the force, spring and damping terms. The process to determine parameters of PM model such as $K_0, K_1, B_0i, B_1i, B_0d, B_1d, F_0$ and F_1 is necessary before manipulator modeling. Each value of PM model parameters was determined as like Table I by many experiments for this works.

B. Modeling of a Joint

PM's antagonistic configuration is now considered. PM can only contract, so if one side of a pair of PMs is contracted, it has no way to return unless the other one contracts to stretch it. This characteristic requires a pair of PMs for one degree of freedom, such as a link in Fig.1. Final actuator torque from a PM pair is the difference between two PMs. Mathematically, the relation is described as (6).

$$\begin{aligned} x_b &= r(\theta + \frac{\pi}{2}) \\ x_t &= r(\frac{\pi}{2} - \theta) \end{aligned} \tag{4}$$

where θ is from $-\frac{\pi}{2}$ to $\frac{\pi}{2}$ with clockwise positive direction.

$$\begin{aligned} \tau_b &= (F(P_b) - K(P_b)x_b - B_b(P_b)\dot{x}_b)r \\ \tau_t &= (F(P_t) - K(P_t)x_t - B_t(P_t)\dot{x}_t)r \end{aligned} \tag{5}$$

TABLE I
Determined PM's parameters from experiments.

Factor	Parameter	Value
Spring element	K_0	4.82
	K_1	1.31
Damping element	$B_{0i}(B_{0d})$	1.22(1.31)
	$B_{1i}(B_{1d})$	1.35(-2.3)
Force element	F_0	14.89
	F_1	20.9

where τ_b and τ_t mean the torque of bicep and tricep muscle. The parameters of F, K and B is from (2). x_b and x_t are the contraction length of bicep and tricep. r is the radius of joint.

$$\begin{aligned} \tau_{total} &= \tau_b - \tau_t \\ &= (F(P_b) - K(P_b)x_b - B_b(P_b)\dot{x}_b \\ &\quad - F(P_t) + K(P_t)x_t + B_t(P_t)\dot{x}_t)r \end{aligned} \tag{6}$$

Until now a link depends on two input of P_b and P_t. A link is actuated by the torque difference of two muscles, so only the pressure difference can be the unique input. Each pressure input can be set like (7) to match only one input to a link.

$$\begin{aligned} 0 \le (P_b = P_{b0} + \Delta P) \le P_{MAX} \\ 0 \le (P_t = P_{t0} - \Delta P) \le P_{MAX} \end{aligned} \tag{7}$$

$$P_{NP} = P_{b0} - P_{t0} \tag{8}$$

where P_{b0} and P_{t0} are nominal pressures. P_{MAX} is the maximum pressure that compressor can generate in real. Then, $(2\Delta P + P_{NP})$ is the pressure difference between two muscles at given time, and only ΔP become the controllable unique input. P_{NP} is the nominal pressure difference between bicep and tricep. P_{NP} is derived by setting τ_b equal to τ_t at given nominal position. Final torque from PM pairs is described like (9) from (6) to (7).

$$\tau = \tau_0 + \tau_1 \Delta p \tag{9}$$

where τ_0 and τ_1 are described at (10).

$$\begin{aligned} \tau_0 =& [F_1 P_{NP} - 2K_0 r\theta - K_1(P_{b0}x_b - P_{t0}x_t) \\ &- (B_{b0} + B_{b1}P_{b0})\dot{x}_b + (B_{t0} + B_{t1}P_{t0})\dot{x}_t]r \\ \tau_1 =& [2F_1 - K_1 r\pi - B_{b1}\dot{x}_b + B_{t1}\dot{x}_t]r \end{aligned} \tag{10}$$

C. Compliance property of a joint

The key idea in modifying joint compliance is to adjust the nominal pressure of the bicep and tricep at PM actuation. PM's nominal pressure has an effect on the joint stiffness property dominantly without affecting on the joint angle at a constant P_{NP}. A torque by joint's spring force terms is derived as in (11) by extracting spring terms from (10).

$$\begin{aligned}\tau_{s_j} =&\tau_{s_b} - \tau_{s_t} = S_j \cdot \theta \\ =&(K_0 + K_1 P_{b0}) r \cdot x_b - (K_0 + K_1 P_{t0}) r \cdot x_t \\ &+ K_1 (x_b + x_t) r \Delta P\end{aligned} \tag{11}$$

where τ_{s_j} is the spring torque at a joint. τ_{s_b} and τ_{s_t} are spring torque from bicep and tricep. S_j is the stiffness value.

By applying (4) and (8) to (11), spring torque equation is derived like (12).

$$\begin{aligned}\tau_{s_j} &= S_j \cdot \theta \\ &= 2r^2 K_0 \theta + K_1 (r^2 \pi P_{b0} - P_{NP} x_t r) + K_1 r^2 \pi \Delta P\end{aligned} \tag{12}$$

Finally the joint compliance of a joint is derived as in (13).

$$\begin{aligned}C_j &= \frac{1}{S_j} \\ &= \frac{\theta}{2r^2 K_0 \theta + K_1 (r^2 \pi P_{b0} - P_{NP} x_t r) + K_1 r^2 \pi \Delta P}\end{aligned} \tag{13}$$

D. Dynamics of 2-link manipulator with PMs

2-link manipulator's dynamics is a general approach and is well described in many textbook as a form of (14).

$$D(\Theta)\ddot{\Theta} + C(\Theta, \dot{\Theta})\dot{\Theta} + G(\Theta) = \tau \tag{14}$$

where D is a robot inertia matrix, C is a matrix of Coriolis and centrifugal effects and G is a matrix of gravity loading. τ is a torque.

We can derive the dynamics equation of (15) which has the input of pressure and the output of joint acceleration by replacing torque τ of (14) by (9).

$$\begin{aligned}\ddot{\Theta} =& A + G \cdot \Delta P \\ & or \\ \begin{bmatrix} \ddot{\theta}_1 \\ \ddot{\theta}_2 \end{bmatrix} =& A + G \begin{bmatrix} \Delta p_1 \\ \Delta p_2 \end{bmatrix}\end{aligned} \tag{15}$$

where

$$A = \begin{bmatrix} a_1 \\ a_2 \end{bmatrix} = D^{-1}(-C \cdot \dot{\Theta} - G + \begin{bmatrix} \tau_{0_1} \\ \tau_{0_2} \end{bmatrix}) \tag{16}$$

and

$$G = \begin{bmatrix} g_{11} & g_{12} \\ g_{21} & g_{22} \end{bmatrix} = D^{-1} \begin{bmatrix} \tau_{1_1} & 0 \\ 0 & \tau_{1_2} \end{bmatrix} \tag{17}$$

For the above equations, Δp_1 and Δp_2 are ΔP for each link1 and link2. τ_{0_1} and τ_{0_2} are τ_0 for each link1 and link2. τ_{1_1} and τ_{1_2} are τ_1 for each link1 and link2. If we set the nominal pressure as the P_{b0} and P_{t0}, then A and G matrix is directly defined by current joint value and joint velocity.

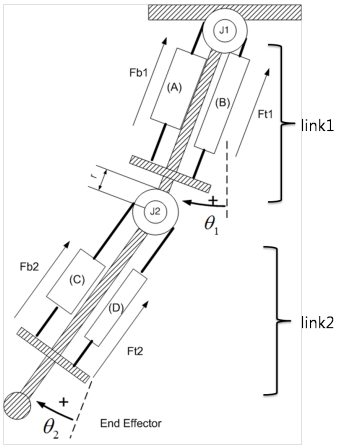

Fig. 1. 2-Link Manipulator schematic. (a) and (c) are PMs of bicep. (b) and (d) are PMs of tricep. A pair of (a) and (b) actuate a joint of J1 and a pair of (c) and (d) actuate a joint of J2.

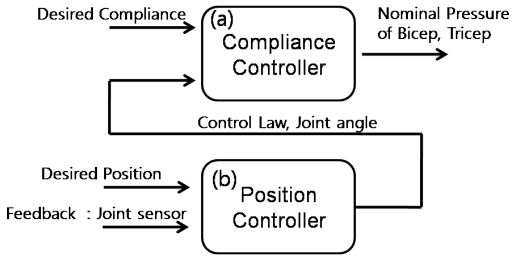

Fig. 2. Whole manipulator controller. (a) is a joint compliance controller(IJCC). (b) is a position controller(SMC).

III. Whole Manipulator Control : Position and Compliance

A whole manipulator controller that consists of position and compliance controller as shown in Fig.2 is proposed. Particularly, the joint compliance is controlled independently of position controller with no affect on position control.

A. Position control

A focus on achieving manipulator elasticity inevitably results in low joint stiffness, which induces low precision in the end-effector due to vibration during movement. Moreover, the A and G matrix of (15) are imprecise terms, which includes PM model parameters with the unavoidable estimation errors. BASMC is used to guarantees the bounded error of the trajectory tracking problem, though it cannot assure optimal tracking with zero error. BASMC is the kind of SMC with the continuous feedback gain to mitigate control law's chattering. It use saturation function instead of signum function for feedback gain.

For each joint i(=1, 2), assume estimate $\hat{a}_i$ of a_i from (15) for known parameter α_i such that

$$|\hat{a}_i - a| \leq \alpha_i \tag{18}$$

Assume the control gain g_i is also unknown but upper and lower bound is known like (19),

$$0 < g_{i_{\min}} \leq g_i \leq g_{i_{\max}} \tag{19}$$

and define

$$\gamma_i = \sqrt{\frac{g_{i_{\max}}}{g_{i_{\min}}}} \tag{20}$$

Let the estimation of g_i as

$$\hat{g}_i = \sqrt{g_{i_{\min}} g_{i_{\max}}} \tag{21}$$

and the sliding surface as

$$\begin{aligned} \sigma_i(t) =& 0, \\ \sigma_i =& \dot{\tilde{\theta}}_i + \mu_i \tilde{\theta}_i, \\ \tilde{\theta}_i(t) =& \theta_i(t) - \theta_i^*(t) \end{aligned} \tag{22}$$

where μ_i are the positive real numbers set by user.

In conclusion we can set the control law or ΔP of (15) as

$$\begin{aligned} \Delta p_i(t) =& \frac{\Delta \hat{p}_i(t) - q_i \cdot sat(\frac{\sigma_i(t)}{T_i})}{\hat{g}_i} \\ \Delta \hat{p}_i(t) =& -\hat{a}_i(t) + \theta_i^*(t) - \mu_i \dot{\tilde{\theta}}_i(t) \\ q_i \geq& \gamma_i(\alpha_i + \varepsilon_i) + (\gamma_i - 1)|\Delta \hat{p}_i| \\ T_i :& \{(\theta_i, \dot{\theta}_i) : |\sigma_i(\theta_i, \dot{\theta}_i)| \leq T_i\} \end{aligned} \tag{23}$$

where T_i is the boundary layer thickness of the sliding surface for each joint i.

B. Compliance control

1) Independent joint compliance control: The proposed controller structure of Fig.2 make it possible to control manipulator's joint compliance independently of position control. It is assumed that $[(P_{b0} = P_{t0}) = P_C]$ by setting the manipulator's nominal position to zero angle usually. Then, the joint compliance are determined like (24) from (13) for each joint $i(= 1, 2)$.

$$C_{j_i} = \frac{\theta_i}{2r^2 K_0 \theta_i + K_1 r^2 \pi (P_{C_i} + \Delta p_i)} \tag{24}$$

At a moment, the joint compliance C_{j_i} depend on only P_{C_i}, because θ_i are from joint sensors and Δp_i are determined by the position controller. Then, the control laws P_{C_i} for the desired joint compliance C_{j_i} are directly determined from (25) without the compliance sensor feedback.

$$P_{C_i} = \frac{\theta_i - r^2(2K_0\theta_i + K_1 \pi \Delta p_i) C_{j_i}}{K_1 r^2 \pi C_{j_i}} \tag{25}$$

$$|\Delta p_i| \leq P_{C_i} \leq P_{MAX} - |\Delta p_i| \tag{26}$$

such that $\forall \theta_i \in (-\frac{\pi}{2}, \frac{\pi}{2})$ and $\forall C_{j_i} \in (C_{i_{MIN}}, C_{i_{MAX}})$, where $C_{i_{MIN}}$ and $C_{i_{MAX}}$ are determined as (27) by applying (26) to (24). $C_{i_{MAX}}$ are at $(P_{C_i} = |\Delta p_i|)$ and $C_{i_{MIN}}$ are at $(P_{C_i} = P_{MAX} - |\Delta p_i|)$. P_{C_i} are limited by (26) from rearranged (7) for both bicep and tricep.

$$\begin{aligned} C_{i_{MIN}} &= \frac{|\theta_i|}{2r^2 K_0 |\theta_i| + 2K_1 r^2 \pi P_{MAX}} \\ C_{i_{MAX}} &= \frac{|\theta_i|}{2r^2 K_0 |\theta_i| + 2K_1 r^2 \pi |\Delta p_i|} \end{aligned} \tag{27}$$

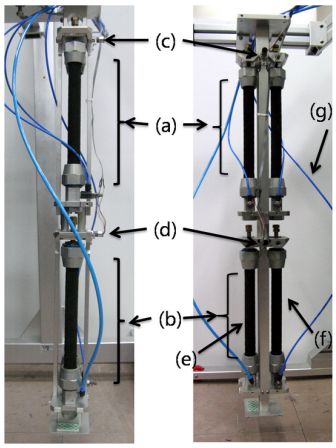

Fig. 3. The schematic of the PMR. The left is the front view and the right is the side view. (a) is a link1 and (b) is link2. (c) and (d) are encoders of the joint1 and joint2. (e) and (f) are PMs of bicep and tricep. (g) is a air hose.

2) Compliance control for the safety characteristic: Here, we aim to maximize the joint compliance for the safety purpose, so the joint compliance control law P_{C_i} are determined as (28).

$$\text{Safety constraint} : P_{C_i} = |\Delta p_i| \tag{28}$$

In that case, the joint compliance are estimated as $C_{i_{MAX}}$ and the final pressure inputs to each side are determined as (29) by (7) and (28).

$$\begin{aligned} P_{b_i} &= \Delta p_i \cdot (\text{sgn}(\Delta p_i) + 1) \geq 0 \\ P_{t_i} &= \Delta p_i \cdot (\text{sgn}(\Delta p_i) - 1) \geq 0 \end{aligned} \tag{29}$$

This is the special one-side actuation control strategy for safety constraint.

IV. Experiment

The proposed method was examined on the real robot of Pneumatic Muscle Robot(PMR). PMR realized the reverse actuation mechanism of Fig.1. Joint1 of (c) is actuated by PMs of the part (a) and Joint2 of (d) by PMs of the part (b) in Fig.3. 2 encoders are attached at each joint for position feedback, there are 4 pneumatic muscles for 2 revolutionary joints, 4 external proportional pressure regulators for individual pneumatic actuators and 1 air compressor. The FESTO company's $20mm$ diameter pneumatic air muscles are used as actuators. Also, the control board that consists of an AVR MCU with a 10 bit and 4 channels DAC whose outputs are inputs to the proportional pressure regulators was developed. The control frequency was set to 60Hz. Developed PMR's dimension is listed in Table II.

where Link1 and Link2 are the length of the each link, LinkC1 and LinkC2 are the length from joint to the center of mass point of the each link.

In experiments, the nominal pressures of static $225kPa$ common to all joints were used as a comparing condition.Maximum pressure of 450kPa was allowed for both bicep and tricep PM in this experiment. The most wide

TABLE II

2-LINK MANIPULATOR KINEMATIC INFORMATION

Parameter	Value	Parameter	Value
Link1	0.5m	Link2	0.5m
LinkC1	0.25m	LinkC2	0.25m
Link1 weight	2Kg	Link2 weight	2Kg
Joint1 radius	0.035m	Joint2 radius	0.035m

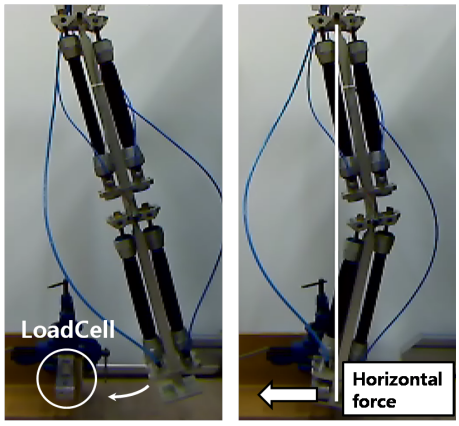

(a) T(-0.34, -0.36) (b) Collision at 11.95s

Fig. 4. Still shots of the collision experiment. Manipulator collide against to the loadcell at 11.95s.

operational range is acquired when $P_{C_{1,2}}$ are the middle of maximum pressure. This is the conventional method to control PMs with no consideration of joint compliance control. In addition, PBSMC was compared with the proposed method. PBSMC is kind of SMC to increase joint compliance. It suppose imaginary object, called proxy, to the robot's end effector by means of virtual spring-coupling. Essentially, conventional SMC control the proxy's position and real end effector is forced to move to proxy by virtual spring-coupling. Virtual spring-coupling give joints increased compliance. Impact impulses that determined by (30) are used to estimate the safety of robot.

$$I = \int_{t_0}^{t_f} F dt \tag{30}$$

where I means impulse during collision and F means force to the object. t_0 is the collision moment and t_f is the end of collision.

The experimental environment pictured in Fig.4 was constructed to measure impacts impulses. The load-cell was positioned on the floor near the projection of the joint1. At that point, the horizontal direction impulses were only measured using a load-cell from a general assumption of a obstacle's horizontal movement like human. The direction of impact impulses and the direction of obstacle's movement are the same. The standard value of a load-cell for a unit weight was decided by hanging a dumbbell of $10Kg$.

$$\begin{aligned} Joint1 &: 0.5 \times sin(t) \\ Joint2 &: 0.5 \times \cos(t) \end{aligned} \tag{31}$$

The manipulator's motion was given of (31), and it could not reach the desired position due to colliding against the load-cell at 11.95s. The impulses were measured for a moment of 0.16s in the cases of the normal condition of ($P_{C_{1,2}} = 225kPa$), the safety constraint and PBSMC. The measured forces are shown in Fig.6. Impact impulses were decreased to $5.23Ns$ with the proposed method comparing to $5.42Ns$ at PBSMC and $7.85Ns$ at a normal configuration of ($P_{C_{1,2}} = 225kPa$). This experiment showed that almost 33% of the impact impulses were decreased at the proposed safety constraint with IJCC, comparing to the normal operational condition. PBSMC's safety performance was almost same to the proposed method, but its tracking performance was more lower than the proposed one owing to PBSMC's virtual spring-coupling as depicted in Fig.5. The impact impulses at the safety constraint were decreased by virtue of the increased joint compliance of Fig.7.

Midpoints of $150kPa$ and $300kPa$ of $P_{C_{1,2}}$ were also accessed by the interval of $25kPa$, which is displayed in Table III. The experimental results from the various $P_{C_{1,2}}$ showed that the lower $P_{C_{1,2}}$ were, the lower the impact impulses were at collisions. However, proposed method maximized the joint compliance resulting in the smallest impulses with a full swing of $\Delta p_{1,2}$. Increased compliance by decreasing $P_{C_{1,2}}$ as is in the conventional approach result in limited motion range.

Mean squared errors(MSE) during [$1s$(settling time) $\sim$ $11.95s$(collision time)] were derived to measure only tracking performance in Table III. Notably, there were not much increase of MSE of joint positions as $P_{C_{1,2}}$ decrease with IJCC contrary to PBSMC's large errors. In conclusion, the safety characteristic was enhanced with the proposed method without much loss of positioning performance.

TABLE III

MEASURED IMPACT IMPULSE AND MSE AT COLLISION EXPERIMENTS

$P_{C_{1,2}}(kPa)$	Impulses(Ns)	MSE of (Joint1, Joint2)
300	12.87	(0.00039, 0.00038)
275	11.81	(0.00038, 0.00039)
250	9.02	(0.00042, 0.00041)
225	7.85	(0.00043, 0.00042)
200	7.21	(0.00044, 0.00042)
175	6.62	(0.00046, 0.00043)
150	6.36	(0.00048, 0.00045)
* $\lvert\Delta p_{1,2}\rvert$ with IJCC	5.23	(0.00051, 0.00047)
PBSMC	5.42	(0.00091, 0.027)

V. CONCLUSION

It is a fundamental proposition that a robot must never injure a human, and they are considered to be safer when they offer greater joint compliance. In relation to this, a joint compliance control method without significant loss of precision performance in the manipulator was addressed in the present work. PMs with intrinsic elasticity were used as basic actuators with an antagonistic configuration. The proposed unified control framework with IJCC and SMC for the manipulator actuated by PMs was utilized to meet safety

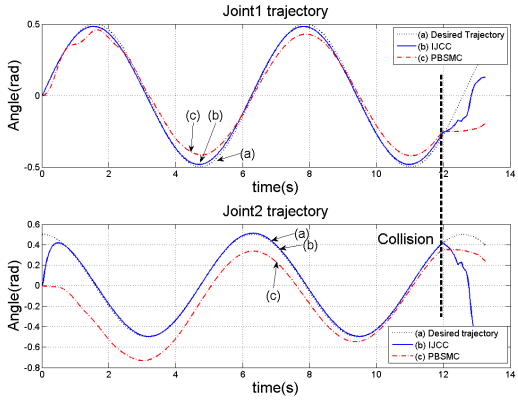

Fig. 5. Position variations at collision experiments with the safety constraint and IJCC. It shows good tracking performance before collisions.

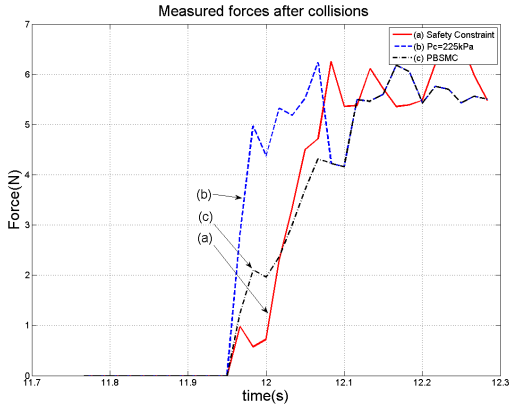

Fig. 6. Measured forces at collision experiments. Proposed the safety constraint with IJCC and PBSMC show low forces after collisions.

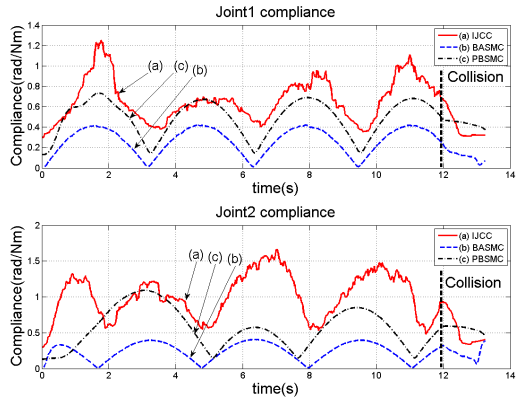

Fig. 7. Estimated compliance variations at collision experiments. The compliance at the safety constraint shows more increased joint compliance (3.0∼3.4 times of the case of ($P_{C_{1,2}} = 225kPa$) depending on the position).

characteristics. The suggested model presented enhanced safety relative to conventional works at collision experiments.

REFERENCES

[1] James H. Graham, John F. Meagher, Stephen J. Derby "A Safety and Collision Avoidance System for Industrial Robots," *IEEE Trans. on Industrial Electronics*, vol. IA-2, no. 1, pp. 195-203, Feb. 1986.

[2] B. Karlsson, N. Karlsson, P. Wide "A dynamic safety system based on sensor fusion," *Journal of Intelligent Manufacturing*, vol. 11, pp. 475-483, 2000.

[3] Eijiro Ohashi, Takahiro Aiko, Toshiaki Tsuji, Hiroaki Nishi, Kouhei Ohnishi "Collsion Avoidance Method of Humanoid Robot With Arm Force," *IEEE Trans. on Industrial Electronics*, vol. 54, no. 3, pp. 1632-1641, Jun. 2007.

[4] Zinn, M., Khatib, O., Roth, B., Salisbury, J.K., "Playing it safe [human-friendly robots]," in *IEEE Robotics & Automation Magazine*, vol. 11, issue 2, pp. 12-21, Jun. 2004.

[5] G. Hirzinger, A. Albu-schäffer, M. Hähnle, I. Schaefer, N. Sporer, "A new generation of torque controlled light-weight robots," in *Proc. Int. Conf. Robotics Automation*, Seoul, Korea, 2001, pp. 3356-3363.

[6] G. Pratt and M. Williamson, "Series elastic actuators," in *Proc. IEEE Int. Conf. Intelligent Robots and Systems*, vol. 1, pp. 399-406, 1995.

[7] Richard Q. van der Linde, "Design, Analysis, and Control of a Low Power Joint for Walking Robots, by Phasic Activation of Mckibben Muscles," *IEEE Trans. on Robotics and Automation*, vol. 15, no. 4, pp. 599-604, Aug. 1999.

[8] Martijn Wisse, Arend L. Schwab, Richard Q. van der Linde, Fran C. T. van der Helm, "How to Keep From Falling Forward: Elementary Swing Leg Action for Passive Dynamic Walkers," *IEEE Trans. on Robotics*, vol. 21, no. 3, pp. 393-401, Jun. 2005.

[9] Ikuo Mizuuchi, Hironori Waita, Ikuo Mizuuchi, Yuto Nakanishi, Tomoaki Yoshikai, Masayuki Inaba, Hirochika Inoue, "Desing and Implementation of Reinforceable Muscle Humanoid," in *Proc. IEEE Int. Conf. Intelligent Robots and Systems*, pp. 828-833, Sep. 2004.

[10] Yoshinao Sodeyama, Ikuo Mizuuchi, Tomoaki Yoshikai, Yuto Nakanishi, Masayuki Inaba, "A Shoulder Structur of Muscle-Driven Humanoid with Shoulder Blades," in *Proc. IEEE Int. Conf. Intelligent Robots and Systems*, pp. 1077-1082, Apr. 2005.

[11] Thomas G. Sugar, Jiping He, Edward J. Koeneman, James B. Koeneman, Richard Herman, H. Huang, Robert S. Schultz, D. E. Herring, J. Wanberg, Sivakumar Balasubramanian, Pete Swenson, Jeffrey A. Ward, "Design and Control of RUPERT: A Device for Robotic Upper Extremity Repetitive Therapy," *IEEE Trans. Neual Systems and Rehabilitation Engineering*, vol. 15, no. 3, pp. 336-346, Sep. 2007.

[12] John H. Lilly, Peter M. Quesada, "A Two-Input Sliding-Mode Controller for a Planar Arm Actuated by Four Pneumatic Muscle Groups," *IEEE Trans. Neual Systems and Rehabilitation Engineering*, vol. 12, no. 3, pp. 349-359, Sep. 2004.

[13] M. Van Damme, B. Vanderborght, R. Van Ham, B. Verrelst, F. Daerden, D. Lefeber, "Proxy-Based Sliding Mode Control of a Manipulator Actuated by Pleated Pneumatic Artificial Muscles," in *Proc. IEEE Int. Conf. Robotics and Automation*, pp. 4355-4360, Roma, Italy, Apr. 2007.

[14] Harald Aschemann, Dominik Schindele, "Sliding-Mode Control of a High-Speed Linear Axis Driven by Pneumatic Muscle Actuators," *IEEE Trans. on Industrial Electronics*, vol.55, no. 11, pp. 3855-3864, Nov. 2008.

[15] Glenn K. Klute, Blake Hannaford, "Accounting for Elastic Energy Storage in McKibben Artificial Muscle Actuators," *Journal of Dynamic Systems, Measurement, and Control*, vol. 122, pp. 386-388, Jun. 2000.

[16] D. B. Reynolds, D. W. Repperger, C. A. Phillips, G. Bandry, "Modeling the Dynamic Characteristics of Pneumatic Muscle," *Annals of Biomedical Engineering* , vol. 32, pp. 310-317, 2003.

[17] Deepak Trivedi, Amir Lotfi, Christopher D. Rahn, "Geometrically Exact Models for Soft Robotic Manipulators," *IEEE Trans. on Robotics*, vol. 24, no. 4, pp. 773-780, Aug. 2008.

[18] Ryo Kikuuwe and Hideo Fujimoto, "Proxy-Based Sliding Mode Control For Accurate and Safe Position Control," in *Proc. IEEE Int. Conf. Robotics & Automation*, pp. 25-30, Orlando, Florida, May, 2006.